

Photophysical and Photochemical Behavior of the Three Conformational Isomers of *trans*-1,2-di(2-Naphthyl)ethene in Nonpolar Solvent

G. Bartocci and A. Spalletti*

Dipartimento di Chimica, Università di Perugia, 06123 Perugia, Italy

Received: January 30, 2002; In Final Form: May 17, 2002

The combined temperature and excitation wavelength effects on the photophysical (fluorescence quantum yields and lifetimes) and photochemical behavior of the rotamer mixture of *trans*-1,2-di(2-naphthyl)ethene (*trans*-2,2'-DNE) has been investigated in nonpolar solvent. By using a refined procedure of the principal component analysis (PCA), applied to the fluorescence spectra of the rotamer mixture, the spectral properties and the relative abundances of the three distinct rotamers at room temperature were derived. Furthermore, the rate constants of their radiative and reactive processes were obtained, so suggesting a complete picture of all of the deactivation pathways of the lowest excited singlet state of the *trans*-2,2'-DNE rotamers.

Introduction

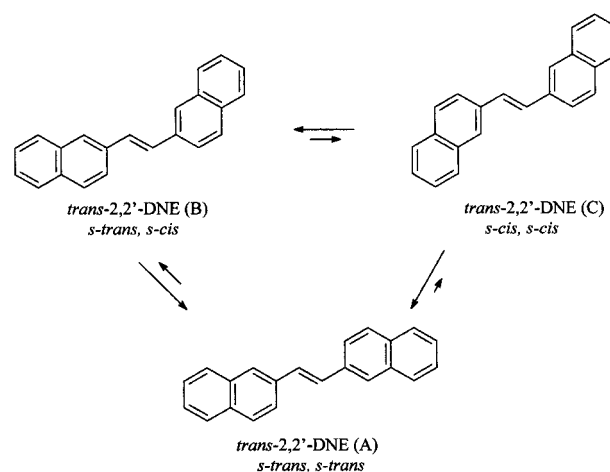
Flexible molecules containing double bonds, as 1,2-diaryl-ethenes, can be found in fluid solution as a mixture of different conformational geometries (rotamers) that exist in dynamic equilibrium in the ground state.^{1,2} In the excited state, the interconversion among the rotamers is often too slow compared to the other deactivation channels of the lowest singlet and triplet excited states leading to noninterconverting excited rotamers (NEER principle)³ with different structures and spectral, photophysical, and photochemical properties. Consequently, one can observe a dependence of the photophysical and photochemical behavior of the rotamer mixture on the excitation wavelength (λ_{exc}).

Kinetic (KFA)⁴ and/or statistical (PCA-SM)^{5,6} procedures were used to obtain the spectral (excitation and emission spectra) and photophysical (fluorescence quantum yields and lifetimes) properties of the pure rotamers by analysis of fluorescence spectra of their mixtures.

In fluid solution at room temperature, *trans*-1,2-di(2-naphthyl)ethene (*trans*-2,2'-DNE) results to be a mixture of three rotamers,^{5b,5c,7–9} whose excitation and emission spectra were derived by Saltiel et al. by a PCA-SM treatment of the fluorescence spectra measured as a function of λ_{exc} at different oxygen and CCl₄ concentrations.⁹ Evidences for at least two rotamers have also been found in the excitation and emission fluorescence spectra of *trans*-2,2'-DNE in crystalline matrixes at 4 K.¹⁰ The *trans* → *cis* quantum yield of the rotamer mixture ($\phi_{t \rightarrow c}$) was found to be a function of temperature in methylcyclohexane/2-methylpentane mixtures (MCH/2MP),^{8a} and the fluorescence decay was expressed by a sum of at least two exponentials at room temperature.^{8b}

We were intrigued by these interesting results, which are nevertheless widely incomplete, because the excited-state properties of the distinct rotamers were not derived. The aim of this paper is then to extend and complete the study of the spectral, photophysical and photochemical behavior of the rotamer mixture in order to derive all of the kinetic parameters

SCHEME 1



of the deactivation processes of the lowest excited singlet state of the three rotamers of *trans*-2,2'-DNE.

A combined kinetic and statistical procedure (KSFA) has been developed, based on the analysis of fluorescence (spectra, quantum yields and lifetimes) and photoreactive properties of the rotamer mixture as a function of λ_{exc} and temperature.^{6,11} This method allows us to obtain the spectral and photophysical properties of the distinct rotamers and also their fractional contributions in the S₁ state, which are necessary to derive a complete picture of their deactivation channels.

This KSFA procedure is here applied to the fluorescence and *trans* → *cis* photoisomerization of rotamer mixtures of *trans*-2,2'-DNE as a function of λ_{exc} and temperature in nonpolar solvent. The derived photophysical and photochemical properties of the three conformational isomers of *trans*-1,2-di(2-naphthyl)ethene are reported.

Experimental Section

The compound investigated (see Scheme 1) was kindly supplied by the late Professor E. Fischer. The solvent used was a mixture of methylcyclohexane/3-methylpentane (MCH/3MP, 9/1 v/v); some measurements were also carried out in isopentane,

* To whom correspondence should be addressed. E-mail: faby@phch.chm.unipg.it.

TABLE 1: Excitation Wavelength Effect on the Fluorescence ($\bar{\phi}_F$) and *trans* \rightarrow *cis* Photoisomerization ($\bar{\phi}_{t-c}$) of the Rotamer Mixture of *trans*-2,2'-DNE in MCH/3MP at 293 K

λ_{exc} (nm)	$\bar{\phi}_F$	$\bar{\phi}_{t-c}$
313	1.0	0.040
355	0.84	0.060
366	0.73	0.059
374	0.70	0.14

TABLE 2: Fluorescence Decay Parameters of *trans*-2,2'-DNE at Different Excitation and Emission Wavelengths in MCH/3MP at 293 K^a

λ_{exc} (nm)	λ_{em} (nm)	$\bar{\tau}_F$ (ns)	τ_{F1} (ns)	τ_{F2} (ns)	τ_{F3} (ns)	% (2)
330	>340 ^b	4.4		1.9	7.1	20
340	355	5.4		1.9	7.4	35
368	>380 ^b	1.9	1.3	2.2		84
372	>380 ^b	1.9	1.3	2.3		75
376	>380 ^b	1.7	1.5	2.0		39
378	>380 ^b	1.6				

^a The corresponding weight (%) is also reported. ^b Obtained by using cutoff filters.

toluene, tetrachloromethane (CCl₄), and 1-bromonaphthalene (Br-naphthalene). All of the solvents were from Fluka chemical of RPE grade and purified by standard procedures. The solutions were deaerated by purging with nitrogen.

Because the *trans* \rightarrow *cis* photoisomerization was found to be peculiar to the C rotamer of *trans*-2,2'-DNE at least at room temperature (see below), the $\bar{\phi}_{t-c}$ experimental values were corrected taking into account the fraction of absorbed quanta by the other rotamers (A and B conformational isomers, see Scheme 1) at the used excitation wavelengths and temperatures.

The uncertainty in the reported parameters is about 10, 5, and 7% for $\bar{\phi}_{t-c}$, fluorescence quantum yield ($\bar{\phi}_F$), and lifetime (τ_F), respectively.

PM3 semiempirical molecular-orbital calculations were performed using HYPERCHEM software. The geometry of the substrates was optimized using a 3-21 ab initio method (Gaussian 94).¹² The transition energies and oscillator strengths were calculated by the ZINDO module (INDO/1 method) of the CERIU² 3.8 (MSI) package.¹³

Other experimental details of the fluorimetric and photochemical measurements¹⁴ and of the PCA fluorimetric procedure^{6,11} are reported elsewhere.

Results and Discussion

The experimental fluorescence and *trans* \rightarrow *cis* photoisomerization quantum yields of *trans*-2,2'-DNE depend on λ_{exc} at room temperature in MCH/3MP: in fact $\bar{\phi}_F$ changes from 1.0 to 0.70 at λ_{exc} of 313 and 374 nm, respectively, whereas $\bar{\phi}_{t-c}$ changes from 0.042 to 0.14 at the same wavelengths, respectively (see Table 1).

Photophysical Behavior. Poli-exponential fluorescence decay curves were obtained and analyzed as a function of λ_{exc} and λ_{em} at room temperature (see Table 2) in order to obtain (a) the contribution of each rotamer [%(*i*)] to the total decay, whose value also depends on the relative position of their absorption and emission spectra, and (b) the lifetimes of the components.⁴ Owing to the complexity of this system, useful information was obtained by selective analysis of the fluorescence decay of the rotamer mixture. The fluorescence decay was found to be biexponential at $\lambda_{exc} \leq 360$ nm with short (1.9 ns) and longer (7.2 ns) lifetimes in agreement with previous results.^{8b} Excitation at the long-wavelength edge of the absorption band ($\lambda_{exc} \geq 360$ nm) led to a biexponential decay with $\tau_{F1} = 1.4$ ns and $\tau_{F2} =$

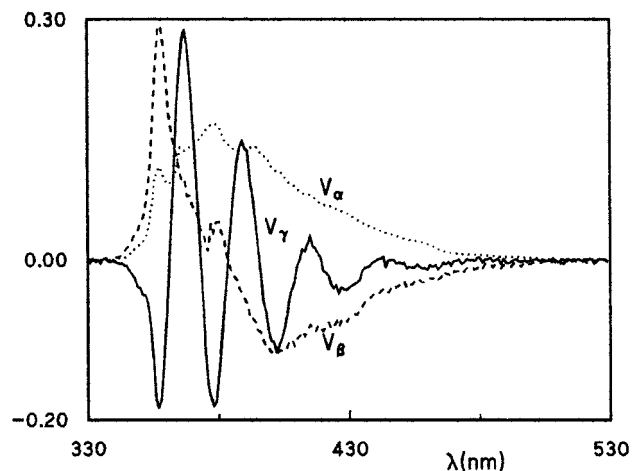


Figure 1. V_α , V_β , and V_γ eigenvectors of the *trans*-2,2'-DNE matrix, obtained from a set of fluorescence spectra in MCH/3MP at 293K as a function of λ_{exc} .

2.2 ns, differently from previous results, which showed a monoexponential decay (2.1 and 1.7 ns at λ_{exc} of 369 and 373 nm, respectively).^{8b}

The present analysis of the fluorescence decay curves allows us to assign the longest-lived (τ_{F3}) component to the hypsochromic component (rotamer A), whereas τ_{F2} and the shortest-lived lifetime (τ_{F1}) are assigned to the B rotamer and the bathochromic C rotamer, respectively.

The dependence of $\bar{\phi}_F$ and $\bar{\phi}_{t-c}$ on λ_{exc} may be explained by the presence in fluid solution at room temperature of a mixture of rotamers; consequently, the $\bar{\phi}_{t-c}$ values can be expressed (eq 1) as the sum of the contribution of each rotamer to the photoisomerization from the following:

$$\bar{\phi}_{t-c}(\lambda_{exc}) = \sum [f_i(\lambda_{exc}) \phi_{t-c,i}] \quad (1)$$

where the subscript *i* refers to the A, B, and C rotamers and the $f_i(\lambda_{exc})$ values are the fractions of excited molecules belonging to each species. Similarly, the fluorescence quantum yield of the rotamer mixture can be expressed as

$$\bar{\phi}_F(\lambda_{exc}) = \sum [f_i(\lambda_{exc}) \phi_{F,i}] \quad (2)$$

The fraction of excited molecules of each rotamer can then be related to the respective fractional contributions $X_i(\lambda_{exc})$ derived by a statistical analysis of the fluorescence data as a function of λ_{exc} (see below) by

$$X_i(\lambda_{exc}) \bar{\phi}_F(\lambda_{exc}) = f_i(\lambda_{exc}) \phi_{F,i} \quad (3)$$

To obtain the $X_i(\lambda_{exc})$, $f_i(\lambda_{exc})$, and $\phi_{F,i}$ values, the KSFA procedure was applied to a series of fluorescence spectra of dilute solutions (absorbance ≤ 0.08) of *trans*-2,2'-DNE in MCH/3MP at room temperature, obtained as a function of λ_{exc} in the 280–380 nm region. The emission intensities were the elements of a 51×200 data matrix. The PCA-SM procedure indicated only three significant components by using the NIPALS algorithm with cross-validators estimation (CVE; double cross procedure).¹⁵

Figure 1 shows the three significant eigenvectors V_α , V_β , and V_γ , which account 99.86% (97.57, 1.91, and 0.38%, respectively) of the total variance of the measured spectra.

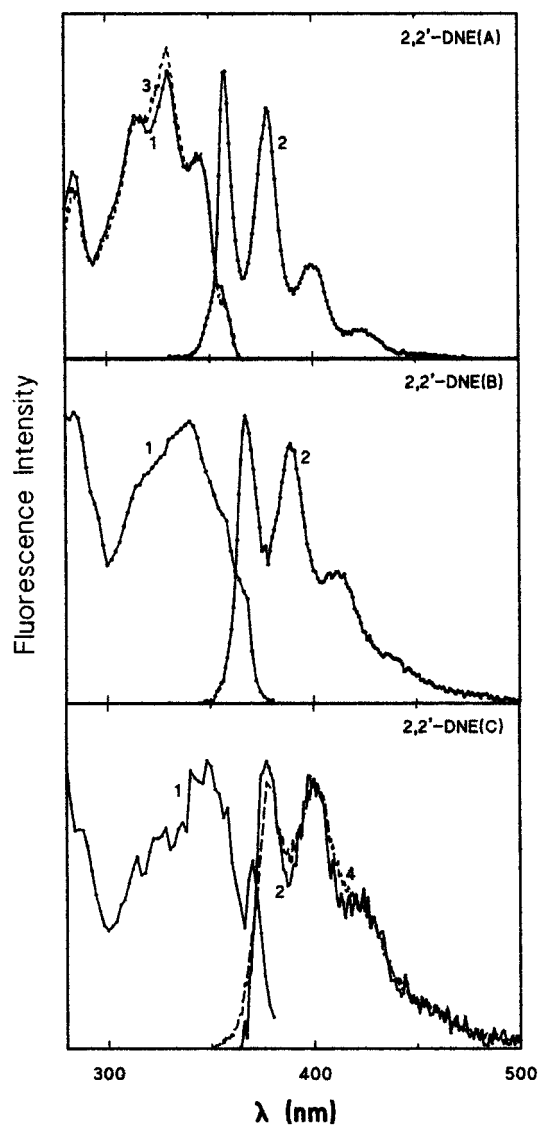


Figure 2. Normalized excitation (curve 1) and emission (curve 2) fluorescence spectra of the three rotamers of *trans*-2,2'-DNE in MCH/3MP at 293 K, as derived by the PCA-SM method. The dashed lines represent the experimental excitation (curve 3) and emission (curve 4) spectra richer in the A ($\lambda_{\text{em}} = 355$ nm) and C ($\lambda_{\text{exc}} = 380$ nm) rotamers, respectively.

The fluorescence spectra of the three rotamers, as derived by eq 4

$$\mathbf{S}_i = \alpha_i \mathbf{V}_\alpha + \beta_i \mathbf{V}_\beta + \gamma_i \mathbf{V}_\gamma \quad (4)$$

are shown in Figure 2. The coefficients of the pure components (α_i , β_i , and γ_i) were derived from the procedure described in a previous work.⁶ The emission maxima of the conformers are shown in Table 3. The emission spectrum of the bathochromic species (C rotamer), derived by the PCA-SM procedure overlaps that obtained by selective excitation ($\lambda_{\text{exc}} = 380$ nm; see Figure 2), so supporting the reliability of this statistical procedure. The energies of the emission spectra, found for the three rotamers, are in good agreement with Saltiel's results obtained by the PCA-SV procedure,⁹ even if, in the latter case, the distribution of the intensities is a little different, particularly for the C rotamer.

The fluorescence spectrum of all of the three rotamers displays the same vibronic structure with a progression of about 1450 cm^{-1} . The structured emission spectra indicate that the fluorescence originates from a relaxed "quasiplanar" geometry.

TABLE 3: Calculated and Experimental Energies of the S_1 State and Oscillator Strengths (f) of the Three Rotamers of *trans*-2,2'-DNE

rotamer	absorption			emission	
	energies			energies	
	expt ^a (nm)	calcd ^b (nm)	f	expt ^a (nm)	expt ^c (nm)
2,2'-DNE(A)		282	1.07		
	314			358	361
	329	328	0.006	378	382
	345	345	1.46	400	404
2,2'-DNE(B)	356 ^{sh}			424	423 ^{sh}
		282	1.05		
	316 ^{sh}	302	0.30	368	371
		328	0.008	389	392
	340	353	1.05	412	415
2,2'-DNE(C)	358 ^{sh}				449 ^{sh}
	366 ^{sh}				
		281	1.28	377	382 ^{sh}
	325 ^{sh}	328	0.013	399	401
	348	358	1.06	423	421
	370				

^a Present work, by PCA-SM procedure. ^b Present work, by INDO/1 method. ^c From ref 5c.

The ratio between the fractional contributions of each component, $X_i(\lambda_{\text{exc}})$, and the respective normalization factor, $N(\lambda_{\text{exc}})$, $X_i(\lambda_{\text{exc}})/N(\lambda_{\text{exc}})$ are given in Table 4 at each λ_{exc} , together with the experimental $\bar{\phi}_F(\lambda_{\text{exc}})$ values. The distribution of the $X_i(\lambda_{\text{exc}})/N(\lambda_{\text{exc}})$ values, as a function of λ_{exc} , represents the excitation spectrum of each pure rotamer (see Figure 2).

The absorption properties of the three rotamers of *trans*-2,2'-DNE, derived by the PCA procedure, are shown in Table 3 together with the excitation energies and oscillator strengths for the singlet states, calculated by the ZINDO module (INDO/1 method).

For all of the three conformers, these calculations show an ethenic nature of the first excited singlet state and a naphthalenic character of the S_2 state with low oscillator strength. In contrast, CNDO/S calculations showed that the two rotamers of the asymmetric analogue (*trans*-2-styrylnaphthalene) have a different character of the S_1 state: L_b and (L_a-B_u) for the longer-living and more stable (B rotamer) and short-lived (A rotamer) species, respectively.¹⁶ The derived excitation spectra of all of the three rotamers show a strong band in the 300–375 nm spectral region, with little vibrational structure. Furthermore, it seems to be due to a combination of two main overlapped bands. The first one, more intense, located in the 300–350 nm region, is probably of ethenic type, owing to the characteristic vibronic structure with $\Delta\bar{\nu} = 1450 \text{ cm}^{-1}$, as shown by the excitation spectrum of the A rotamer (see Figure 2). The second one is observed at the onset (360–370 nm) of the spectra. This hidden band could be of naphthalenic (L_b) or mixed (L_a-B_u) type, as previously found for *trans*-*n*-StNs (see below).¹⁶ The excitation and emission spectra of the A conformation are blue-shifted with respect to those of B and C, in agreement with the previous results obtained in *n*-hexane matrix at 4 K.¹⁰

The lack of Stokes shift between the 0,0 energies of the S_0-S_1 transitions for all of the three rotamers is in agreement with the very low values of the dipole moments of S_0 and S_1 , obtained by calculations (about 0.002 D).

The PCA-SM procedure was also applied to an input matrix (8×200), generated by a set of fluorescence spectra recorded as a function of λ_{exc} in the 365–380 nm range. Only two significant eigenvectors (components) were obtained, which account for 99.39% (97.40% and 1.99%, respectively) of the

TABLE 4: Fluorescence Parameters of *trans*-2,2'-DNE in MCH/3MP at 293 K from the KSFA Method as a Function of λ_{exc}

λ_{exc} (nm)	$\bar{\phi}_{\text{F}}$ (λ_{exc})	$X_{\text{A/N}}$ (λ_{exc})	$X_{\text{B/N}}$ (λ_{exc})	$X_{\text{C/N}}$ (λ_{exc})	f_{A} (λ_{exc})	f_{C} (λ_{exc})	ϕ_{FB}
280	1.0	3.75	7.48	1.31	0.299	0.179	1.14
282	1.0	4.17	7.39	1.15	0.328	0.157	1.13
284	1.0	4.64	7.57	1.02	0.351	0.133	1.11
286	1.0	4.53	7.43	1.03	0.349	0.136	1.11
288	0.85	3.70	6.95	1.02	0.269	0.128	0.84
290	1.0	2.91	6.13	0.952	0.291	0.164	1.12
292	1.0	2.47	5.50	0.836	0.280	0.164	1.12
294	1.0	2.39	5.19	0.722	0.288	0.150	1.11
296	1.0	2.63	4.82	0.647	0.325	0.138	1.11
298	1.0	2.95	4.12	0.579	0.386	0.131	1.12
300	1.0	3.15	3.60	0.556	0.431	0.131	1.13
302	1.0	3.53	3.74	0.577	0.450	0.128	1.13
304	1.0	3.77	3.94	0.597	0.454	0.124	1.12
306	1.0	4.10	4.19	0.676	0.457	0.129	1.13
308	1.0	4.54	4.59	0.701	0.462	0.122	1.12
310	1.0	5.11	4.97	0.778	0.471	0.124	1.13
312	1.0	5.70	5.32	0.844	0.480	0.122	1.13
314	1.0	6.05	5.64	0.901	0.481	0.124	1.13
316	1.0	5.97	5.69	0.817	0.478	0.112	1.11
318	1.0	5.91	5.93	0.825	0.467	0.112	1.11
320	0.97	5.66	5.99	0.925	0.437	0.124	1.05
322	0.95	5.66	6.13	0.987	0.421	0.126	1.00
324	0.92	5.92	6.26	0.987	0.414	0.119	0.936
326	0.90	6.29	6.40	0.999	0.413	0.113	0.889
328	0.88	6.73	6.49	1.03	0.415	0.109	0.841
330	0.89	7.16	6.86	0.934	0.426	0.095	0.853
332	0.89	6.80	6.93	0.956	0.412	0.100	0.860
334	0.85	5.90	6.78	1.02	0.366	0.108	0.800
336	0.85	5.24	6.77	1.06	0.341	0.119	0.815
338	0.85	4.79	6.73	1.02	0.325	0.119	0.821
340	0.94	4.71	7.34	1.30	0.332	0.157	1.01
342	0.94	4.87	7.21	1.27	0.343	0.154	1.01
344	0.94	5.10	6.90	1.25	0.362	0.152	1.01
346	0.90	4.99	6.37	1.24	0.356	0.152	0.926
348	0.91	4.69	6.03	1.35	0.354	0.176	0.967
350	0.91	3.91	5.76	1.32	0.324	0.188	0.978
352	0.86	2.67	5.41	1.21	0.247	0.193	0.893
354	0.85	1.83	5.08	1.19	0.192	0.215	0.899
356	0.82	1.79	4.91	1.08	0.189	0.197	0.843
358	0.73	1.38	4.74	1.13	0.139	0.196	0.718
360	0.70	0.948	3.96	0.744	0.118	0.159	0.679
362	0.73	0.374	3.44	0.767	0.060	0.210	0.751
364	0.73	0.112	3.21	0.678	0.020	0.214	0.766
366	0.73		2.92	0.568		0.205	0.769
368	0.69		2.72	0.793		0.269	0.730
370	0.70		1.36	0.882		0.474	0.808
372	0.70		0.598	0.734		0.665	0.938
374	0.70		0.308	0.545		0.771	1.10
376	0.66		0.168	0.342		0.764	0.920
378	0.61		0.0083	0.205		1.00	
380	0.58		0.0083	0.149		0.95	

total variance of the measured spectra, in agreement with the result that the A rotamer does not absorb at $\lambda_{\text{exc}} \geq 365$ nm. This mathematical procedure of the PCA method, based on the Lawton–Sylvestre nonnegativity constraints,⁶ yields the same spectral properties for the B and C rotamers, thus supporting the reliability of the two PCA-SM methods.

From eq 3, it is possible to obtain the relative absorption spectrum of each rotamer if the $\phi_{\text{F},i}$ values are known. Excitation at the extreme tail of the *trans*-2,2'-DNE absorption spectrum ($\lambda_{\text{exc}} \geq 380$ nm) where the A and B rotamers do not absorb (see Figure 2) allowed the fluorescence quantum yield of the C rotamer (0.58) to be obtained. By eq 3, the $f_{\text{C}}(\lambda_{\text{exc}})$ values of Table 4 in the 366–376 nm region were then derived. Because a value of 1.0 was assumed for the fluorescence quantum yield of A, on the basis of a $\bar{\phi}_{\text{F}}$ value of 1.0 in the 280–318 nm spectral range, also $f_{\text{A}}(\lambda_{\text{exc}})$ in all the spectral region could be

TABLE 5: Temperature Effect on the Photophysical Properties of *trans*-2,2'-DNE(A) in MCH/3MP^a

T (K)	α_{s}	$\tau_{\text{F,A}}$ (ns)	$k_{\text{F,A}}$ (10^8 s ⁻¹)
293	0.252	7.2	1.39
220	0.272	6.2	1.61
200	0.278	5.7	1.75
175	0.284	4.9	2.05
150	0.291	4.4	2.27
120	0.299	3.7	2.70
77	0.309	2.8	3.57

^a The $k_{\text{F,A}}$ values were obtained by $k_{\text{F,A}}(T) = 1/\tau_{\text{F,A}}(T)$, being $\phi_{\text{F,A}} = 1$ (see text).

calculated by using eq 3. As $\sum f_i(\lambda_{\text{exc}}) = 1$, the introduction of the $\phi_{\text{F,A}}$, $\phi_{\text{F,C}}$, and $X_i(\lambda_{\text{exc}})$ values in eq 3 allowed the fractions of the excited molecules of the three rotamers and the ϕ_{FB} values at each λ_{exc} to be derived. The latter are reported in Table 4, with their mean value being 0.97 ± 0.12 .

The relative absorption spectra, $\epsilon_i(\lambda_{\text{exc}}) c_i/\bar{c}$, calculated from $\bar{\epsilon}(\lambda_{\text{exc}})$ and $f_i(\lambda_{\text{exc}})$ values by eq 5

$$\epsilon_i(\lambda_{\text{exc}}) c_i / [\bar{\epsilon}(\lambda_{\text{exc}}) \bar{c}] = f_i(\lambda_{\text{exc}}) \quad (5)$$

are shown in Figure 3.

The radiative rate constant of the three rotamers was derived by the relationship $k_{\text{Fi}} = \phi_{\text{Fi}}/\tau_{\text{Fi}}$; similar values of 1.4×10^8 , 4.6×10^8 , and 4.1×10^8 s⁻¹ were obtained for the A, B, and C rotamers, respectively, (see Table 6). The value of the radiative parameter of A, $k_{\text{F,A}}$, is lower (about three times) than those of B and C, also if the more stable A rotamer has the most planar conformation. This unexpected result suggests that in this “quasiplanar” conformer the fluorescent state has a naphthalenic L_b character. The large oscillator strength of the S₁ → S₀ transition is then due to a vibronic coupling of an allowed S₂ state into the lowest forbidden ¹L_b* state.¹⁷ As a consequence, its oscillator strength markedly depends on the energy gap between the two lowest excited singlet states.

The inversion in the ordering of these excited states of singlet multiplicity in the A rotamer is supported by the effect of solvent polarizability [evaluated from the refractive index (n_{s}) as: $\alpha_{\text{s}} = (n_{\text{s}}^2 - 1)/(n_{\text{s}}^2 + 2)$] on its absorption spectrum (see Figure 4).^{17–19} When α_{s} increased, a red shift of the S₀ → S₂ transition was observed, whereas the S₂–S₁ energy gap decreased and the S₀→S₁ transition became more evident in the excitation of A rotamer. The $\Delta E(S_2-S_1)$ value shows a linear trend with α_{s} (inset of Figure 4). Interestingly, such a correlation allows the experimental conditions (solvent, temperature) to be found at which the inversion in the nature of the lowest excited state occurs. For this conformer, it corresponds to $\alpha_{\text{s}} \geq 0.486$, in agreement with the Muszkat results, which award an ethenic nature to S₁ of the more stable A rotamer in hexane matrix at 4 K.¹⁰

Furthermore, the fluorescence lifetime of this rotamer shows an “anomalous” dependence on temperature, because it decreases with temperature below 250 K (see Table 5). These findings indicate that the k_{F} values increase at lower temperatures, being $\phi_{\text{F,A}} = 1$ already at room temperature. When the temperature changed to 77 K, $k_{\text{F,A}}$ increased more than 4 times, reaching in rigid matrix a value similar to that found for the B and C rotamers, whose S₁ state has a “quasi-pure” ethenic character, in agreement with the fact that their radiative rate parameters are practically independent of temperature. Table 5 shows the trend of the radiative rate constant of 2,2'-DNE(A) with α_{s} in MCH/3MP at different temperatures. In fact, a decrease of temperature leads to an increase of α_{s} , because of an increase of refractive index.

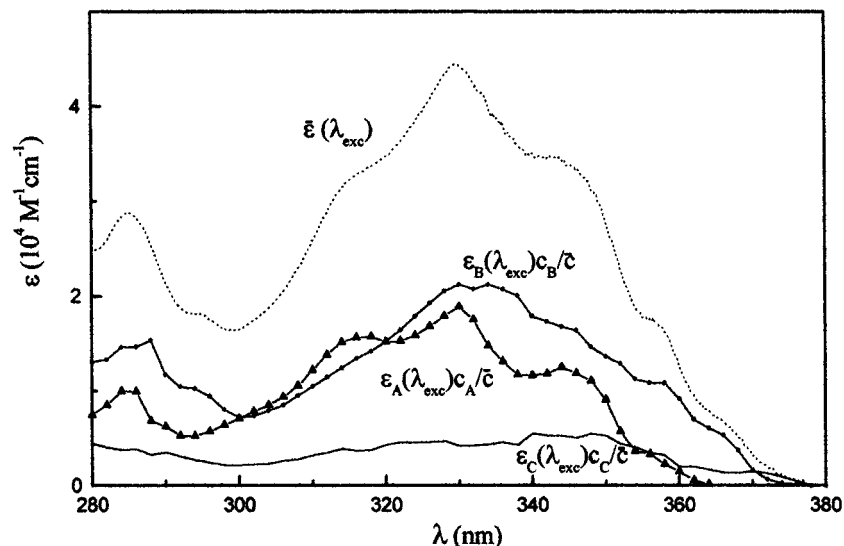


Figure 3. Experimental absorption spectrum $\bar{\epsilon}(\lambda_{exc})$ of *trans*-2,2'-DNE in MCH/3MP at 293 K and relative absorption spectra of the A, B, and C rotamers, $\epsilon_i(\lambda_{exc})c_i/\bar{c}$ ($i = A, B,$ and C), as derived by the KSFA method.

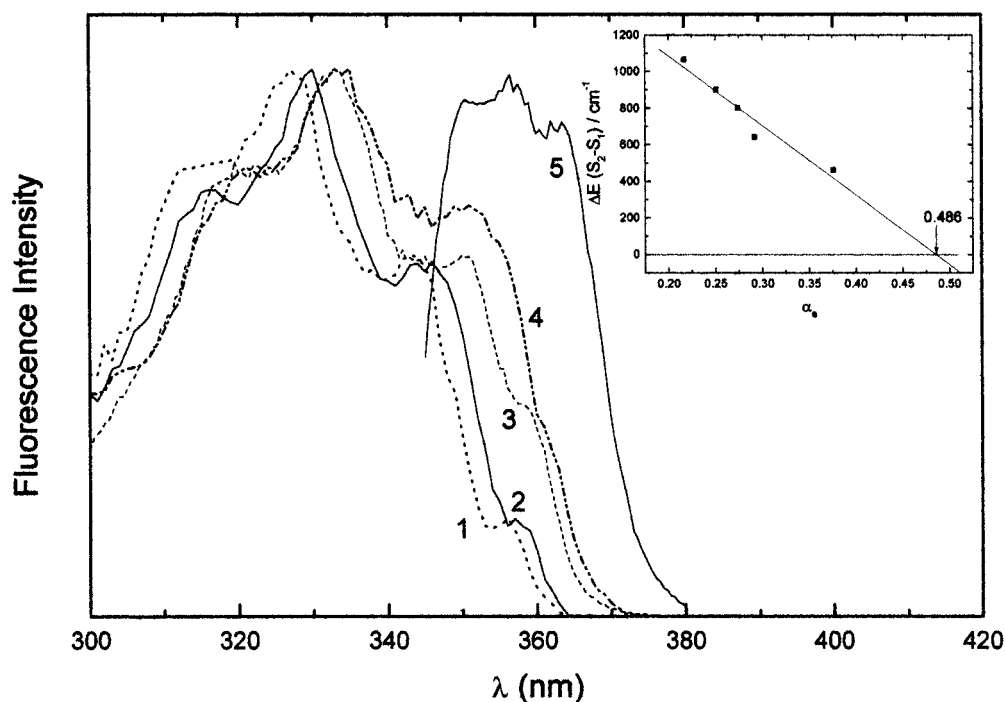


Figure 4. Normalized excitation spectra of *trans*-2,2'-DNE(A) in solvents of different polarizability (1, isopentane; 2, MCH/3MP; 3, toluene; 4, CCl₄; 5, Br-naphthalene) at room temperature. Inset: $\Delta E(S_2-S_1)$ plot as a function of solvent polarizability.

The nonlinear trend of the k_{FA} values with α_s is in agreement with the dependence of k_F on the S_1-S_2 energy gap [$k_F \propto \Delta E(S_1-S_2)^{-2}$], as found for diphenylhexatriene^{18,19} and dithienylpolyenes.¹⁴

An estimate of the standard enthalpy for the $A \rightarrow B \rightarrow C$ interconversion in the ground state can be obtained by assuming that the Franck–Condon envelopes of the first absorption band system (from S_0 to S_1 and S_2) have similar shapes in the three rotamers. It is to be expected from the radiative lifetime relation^{4a} that

$$\epsilon_{0,0}(A)/\epsilon_{0,0}(B) \approx \tau_{FB}^\circ/\tau_{FA}^\circ = \phi_{FA} \tau_{FB}/[\phi_{FB} \tau_{FA}] \quad (6a)$$

$$\epsilon_{0,0}(B)/\epsilon_{0,0}(C) \approx \tau_{FC}^\circ/\tau_{FB}^\circ = \phi_{FB} \tau_{FC}/[\phi_{FC} \tau_{FB}] \quad (6b)$$

The relative abundances in S_0 (0.60, 0.29, and 0.11 for the A, B, and C rotamers, respectively, at room temperature) were then

derived from the ratios $\epsilon_{0,0}(A)c_A/[\epsilon_{0,0}(B)c_B]$ and $\epsilon_{0,0}(B)c_B/[\epsilon_{0,0}(C)c_C]$, estimated from the relative absorption spectra of Figure 3, and by eq 6. From the Boltzmann distribution (neglecting the entropy term), the enthalpy differences among the rotamers were obtained (see Table 6). The results show that the B and C conformational isomers of *trans*-2,2'-DNE lie 1.8 and 4.6 kJ mol⁻¹ above the A rotamer, in reasonable agreement with previous C-INDO calculations.²⁰

Photochemical Behavior. The *trans*-2,2'-DNE shows photoconversion to the cis isomer by direct irradiation in fluid solution at room temperature.^{7,8a} The *trans* \rightarrow *cis* photoisomerization quantum yield, $\phi_{t \rightarrow c}$, depends on λ_{exc} (see Table 1) and, in agreement with previous results,^{7,8a} on temperature (see Table 7).

On the basis of a negligible $S_1 \rightarrow T_1$ intersystem crossing process for *trans*-2,2'-DNE ($\phi_{ISC} < 0.001$)²¹ and of unitary value

TABLE 6: Photophysical and Thermodynamic Parameters of the *trans*-2,2'-DNE Rotamers in MCH/3MP at 293K, Obtained Using the KSFA Method

parameter	DNE(A)	DNE(B)	DNE(C)
ϕ_F	1.0	0.97	0.58
τ_F (ns)	7.2	2.1	1.4
k_F (10^8 s $^{-1}$)	1.4	4.6	4.1
relative abundance in S_0	0.60 (0.53) ^a	0.29 (0.30) ^a	0.11 (0.17) ^a
$\Delta H(S_0)$ (kJ mol $^{-1}$)	1.8 (1.4) ^a	2.8 (1.5) ^a	

^a From ref 20.**TABLE 7: Temperature Effect on the Fluorescence Lifetime of the Rotamers and on the Photoisomerization Quantum Yield of the Rotamer Mixture of *trans*-2,2'-DNE ($\phi_{t \rightarrow c}$) in MCH/3MP at $\lambda_{exc} = 313$ nm^a**

T (K)	$\bar{\phi}_{t \rightarrow c}$	$\tau_{F,1}$ (ns)	$\tau_{F,2}$ (ns)	$\phi_{t \rightarrow c,C}$
248	0.0077			0.088
273	0.016	2.2	7.6	0.15
285	0.033	2.1	7.9	0.30
298	0.040	1.9	7.7	0.33
323	0.072	2.1	7.2	0.41
348	0.11	2.3	6.4	0.44
354		2.0	5.8	

^a The corrected $\phi_{t \rightarrow c}$ for the C rotamer ($\phi_{t \rightarrow c,C}$), derived by eq 8, are also reported at the explored temperatures.

for $(\phi_F + \alpha\phi_{t \rightarrow c})$, where α (about 0.5; for review articles, see ref 22) is the decay fraction from the perpendicular singlet configuration to the cis isomer in the ground state, the photoreactive process is assumed to proceed through a diabatic singlet mechanism.

At any temperature and excitation wavelength, the *trans* \rightarrow cis quantum yield of the rotamer mixture $\bar{\phi}_{t \rightarrow c}(\lambda_{exc}, T)$, can be expressed by eq 7:

$$\bar{\phi}_{t \rightarrow c}(\lambda_{exc}, T) = \sum [f_i(\lambda_{exc}, T) \phi_{t \rightarrow c,i}(T)] \quad (7)$$

Because in a nonpolar solvent at room temperature the radiative process is practically the only deactivation pathway of the S_1 state for the A and B rotamers ($\phi_F \cong 1$ for these conformational isomers, see Table 6), C is the photoreactive species. Considering the fraction of the quanta absorbed by the C conformation at the explored λ_{exc} , one obtains the correct $\phi_{t \rightarrow c}$ values of this rotamer. A mean value of 0.26 ± 0.05 was obtained for $\phi_{t \rightarrow c,C}$ in MCH/3MP at room temperature; it results to be independent of λ_{exc} , so supporting our assumption that this less planar geometry is the only responsible for the cis production at room temperature.

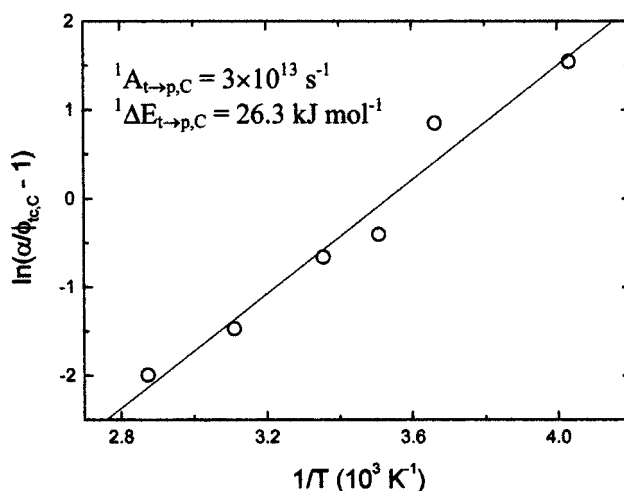
Temperature Effect. Table 7 shows the dependence of $\bar{\phi}_{t \rightarrow c}$ and fluorescence lifetimes on temperature. The $\tau_{F,1}$ values are a mean of the B and C lifetimes, because they are not separable by a three exponential treatment of the decay curves owing to the complexity of the system. $\tau_{F,2}$, assigned to the A rotamer, was independent of temperature up to 320 K; at higher temperatures, it decreased with increasing temperature, thus suggesting the opening of a reactive pathway to the S_1 deactivation of this rotamer.

The Arrhenius parameters of the ${}^1\text{trans}^* \rightarrow {}^1\text{perp}^*$ activated torsional process in the S_1 state can be derived by eqs 8 and/or 9:

$$\ln[\alpha/\phi_{t \rightarrow c,i} - 1] = \ln(k_{F,i}/{}^1A_{t \rightarrow p,i}) + {}^1\Delta E_{t \rightarrow p,i}/RT \quad (8)$$

$$\ln(1/\tau_{F,i}(T) - 1/\tau_{F,i}^{\text{lim}}) = \ln({}^1A_{t \rightarrow p,i} - {}^1\Delta E_{t \rightarrow p,i}/RT) \quad (9)$$

A frequency factor, ${}^1A_{t \rightarrow p}$, and an energy barrier, ${}^1\Delta E_{t \rightarrow p}$, of 4.9×10^{13} s $^{-1}$ and 41.2 kJ mol $^{-1}$, respectively, were obtained by eq 9 for the A rotamer.

**Figure 5.** Plot of eq 8 for the C rotamer in MCH/3MP.**TABLE 8: Kinetic and Arrhenius Parameters and Quantum Yields for Radiative and Nonradiative Deactivation of the *trans*-2,2'-DNE Rotamers in MCH/3MP at 293 K**

parameter	DNE (A)	DNE (B)	DNE (C)
$\phi_{t \rightarrow c}$	0.011		0.25
${}^1\Delta E_{t \rightarrow p}$ (kJ mol $^{-1}$)	41.2		26.3
${}^1A_{t \rightarrow p}$ (10^{13} s $^{-1}$)	4.9		3.0
k_F (10^8 s $^{-1}$)	1.4	4.6	4.1
${}^1k_{t \rightarrow p}$ (10^8 s $^{-1}$)	0.022		6.0

The corrected $\phi_{t \rightarrow c,C}$ values at the explored temperatures are also reported in Table 7. These values were derived by eq 7 and from the $\phi_{t \rightarrow c,A}(T)$ values, derived by the relationship

$$\phi_{t \rightarrow c,A}(T) = \alpha {}^1k_{t \rightarrow p,A}(T) \tau_{F,A}(T) = \alpha {}^1A_{t \rightarrow p,A} \exp({}^1\Delta E_{t \rightarrow p,A}/RT) \tau_{F,A}(T) \quad (10)$$

and from the $f_i(\lambda_{exc}, T)$ values ($i = A$ and C; see eq 5), obtained by the $\Delta H(S_0)$ values of Table 6, considering the molar absorption coefficients temperature-independent in the explored temperature range. The temperature dependence of $\phi_{t \rightarrow c,C}$ indicates the presence of an activated reactive process for this rotamer.

Arrhenius parameters of 3.0×10^{13} s $^{-1}$ and 26.3 kJ mol $^{-1}$ were derived from the plot of eq 8 (see Figure 5) for ${}^1A_{t \rightarrow p}$ and ${}^1\Delta E_{t \rightarrow p}$, respectively, for the C rotamer. A previous value of 10.5 kJ mol $^{-1}$ for the activated torsional process of *trans*-2,2'-DNE had been roughly derived by an Arrhenius-type plot of the experimental photoisomerization quantum yields of the rotamer mixture against temperature.^{8a}

Kinetic Parameters. Table 8 collects the photophysical and photochemical parameters and the rate constants of the deactivation processes of the S_1 state of the three rotamers of *trans*-2,2'-DNE in a nonpolar solvent. The radiative process is the most important deactivation pathway for the more planar A and B conformations. The reactive process becomes competitive with the radiative one for the C rotamer at room temperature ($k_{F,C} \approx {}^1k_{t \rightarrow p,C}$) owing to a lower torsional barrier respect to those of A and B.

The $S_1 \rightarrow T_1$ intersystem crossing and the $S_1 \rightarrow S_0$ internal conversion processes are negligible for all of the three rotamers, as previously found for the naphthyl analogues.^{11,16}

Even if the radiative rate constant is large ($\geq 10^8$ s $^{-1}$) for all of the three rotamers, the nature of their S_1 state is different: in B and C, S_1 has a (L_a-B_u) character, whereas in the A rotamer, at room temperature and in solvents of low polariz-

ability, S_1 has a naphthalenic L_b nature. The large k_F value, derived for A, is then due to mixing between an allowed S_2 state of (L_a-B_u) nature and the lowest forbidden ${}^1L_b^*$ state, as previously observed for the *s-trans* conformation of *trans*-1-(2-naphthyl),2-phenylethene.¹⁶

The rate parameters of the activated torsional process were derived by eqs 8 or 9. For the more stable A rotamer, the ${}^1k_{t \rightarrow p}$ value at room temperature is much lower than that of the radiative rate constant, in agreement with the scarce role of its reactive process. On the contrary, the C rotamer shows a ${}^1k_{t \rightarrow p}$ value similar to its radiative parameter, so indicating that the geometry of the excited singlet state can play a relevant role in driving the deactivation of the S_1 state of these conformational isomers through radiative and/or reactive pathways.

Conclusions

Excitation wavelength and temperature effects on the spectral, photophysical, and photochemical properties of *trans*-2,2'-DNE confirmed the presence of conformational equilibria in the ground state in a nonpolar solvent at room temperature. The useful application of the KSFA method to the fluorescence of the rotamer mixture proved to be particularly interesting, because it allowed the enthalpy differences in the ground state and the excited-state properties of the rotamers to be obtained.

The results confirmed the presence of the three rotamers in dynamic equilibrium in S_0 , which cannot interconvert in the S_1 state, as previously found.^{5,8} This equilibrium plays a relevant role in driving the deactivation channels of their lowest excited singlet state toward radiative and/or reactive pathways.

On the basis of the spectral shapes and photophysical parameters of the rotamers, the following conclusion can be drawn:

(i) The long-lived and hypsochromic A rotamer is the most stable conformational isomer, *s-trans*, *s-trans* geometry, in agreement with previous results;^{5c,10}

(ii) The $\Delta H(S_0)$ values are about 1.8 and 2.8 kJ mol⁻¹ between A and B and between B and C, respectively. These values are in reasonable agreement with those expected from C-INDO calculation (1.4 and 1.5 kJ mol⁻¹ for A-B and B-C rotamers, respectively)²⁰ for internal rotation of one 2-naphthyl group;

(iii) The lowest excited singlet state of the B and C rotamers has a (L_a-B_u) nature with mixed (ethenic and naphthalenic) character, based on the relative absorption spectra and k_F values, as previously found for *trans*-1-StN and the *s-cis* conformation of *trans*-2-StN¹⁶ and for the three rotamers of *trans*-1-(2-naphthyl),2-(6'-quinolyl)-ethene (*trans*-2,6-NQE).¹¹ On the contrary, at room temperature and in solvents with low polarizability, the *s-trans*, *s-trans* conformation has the S_1 state of naphthalenic ${}^1L_b^*$ nature, as previously found for the analogue rotamer of *trans*-2-StN.¹⁶ The mixing of an allowed S_2 state, as ${}^1(L_a-B_u)^*$, into a lowest forbidden state, as ${}^1L_b^*$, leads to rather high k_F value for the forbidden S_0-S_1 transition.¹⁷

(iv) The $S_1 \rightarrow T_1$ intersystem crossing is a negligible deactivation process of S_1 for all of the three rotamers, in agreement with previous results.²¹

In nonpolar solvent at room temperature, the *trans* \rightarrow *cis* photoisomerization is a relevant pathway in the S_1 deactivation only for the C rotamer, and the *cis* isomer is formed by a singlet diabatic mechanism. At high temperatures ($T > 320$ K), the photoisomerization of the A rotamer is also observed.

The torsional barrier for the activated reactive process of the A and C rotamers was derived by Arrhenius plots: a higher

barrier was found for A (41.2 kJ mol⁻¹) relative to C (26.3 kJ mol⁻¹), in agreement with a fast photoisomerization of the latter.

The radiative process is the main deactivation process of the S_1 state for the more planar geometries (A and B) in nonpolar solvent at room temperature, whereas the $S_1 \rightarrow S_0$ internal conversion is a negligible process for all of the three isomers.

Acknowledgment. This research was funded by the Ministero per l'Università e la Ricerca Scientifica e Tecnologica (Rome) and the Perugia University in the framework of the Programmi di Ricerca di Interesse Nazionale (Project: Mechanism of Photoinduced Processes in Organized Systems). A grant from the Italian Consiglio Nazionale delle Ricerche (Rome) is also acknowledged. The authors are grateful to Professor U. Mazzucato for stimulating discussions and D. Pannacci for his technical assistance.

References and Notes

- Mazzucato, U.; Momicchioli, F. *Chem. Rev.* **1991**, *91*, 1679.
- Bartocci, G.; Spalletti, A.; Mazzucato, U. In *Conformational Analysis of Molecules in Excited States*; Waluk, J., Ed.; Wiley-VCH Publisher Inc.: New York, 2000; Chapter 5.
- Vroegop, P. J.; Lugtenburg, J.; Havinga, E. *Tetrahedron* **1973**, *29*, 1393. Jacobs, H. J. C.; Havinga, E. *Adv. Photochem.* **1979**, *11*, 305.
- Birks, J. B.; Bartocci, G.; Aloisi, G. G.; Dellonte, S.; Barigelletti, F. *Chem. Phys.* **1980**, *51*, 113. Bartocci, G.; Mazzucato, U.; Masetti, F.; Aloisi, G. G. *Chem. Phys.* **1986**, *101*, 461.
- (a) Saltiel, J.; Eaker, D. W. *J. Am. Chem. Soc.* **1988**, *106*, 7624. (b) Saltiel, J.; Sears, D. F., Jr.; Mallory, F. B.; Mallory, C. W.; Buser, C. A. *J. Am. Chem. Soc.* **1986**, *108*, 1688. (c) Sun, Y.-P.; Sears, D. F., Jr.; Saltiel, J.; Mallory, F. B.; Mallory, C. W.; Buser, C. A. *J. Am. Chem. Soc.* **1988**, *110*, 6974.
- Cruciani, G.; Spalletti, A.; Bartocci, G. *Z. Phys. Chem.* **1991**, *172*, 227.
- Sheck, Yu. B.; Kovalenko, N. P.; Alfimov, M. V. *J. Lumin.* **1977**, *15*, 157.
- (a) Wismontski-Knittel, T.; Fischer, G.; Fischer, E. *J. Chem. Soc., Perkin Trans. 2* **1974**, 1930. (b) Haas, E.; Fischer, G.; Fischer, E. *J. Phys. Chem.* **1978**, *8*, 1638.
- Sun, Y.-P.; Sears, D. F., Jr.; Saltiel, J. *Anal. Chem.* **1987**, *59*, 2515.
- Muszkat, K. A.; Wismontski-Knittel, T. *J. Phys. Chem.* **1981**, *85*, 3427.
- Bartocci, G.; Spalletti, A.; Masetti, F.; Cruciani, G. *J. Mol. Struct.* **1993**, *165*, 165.
- Frisch, M. J.; Trucks, G. W.; Schlegel, H. B.; Gill, P. M. W.; Johnson, B. G.; Robb, M. A.; Cheeseman, J. R.; Keith, T.; Petersson, G. A.; Montgomery, J. A.; Raghavachari, K.; Al-Laham, M. A.; Zakrzewski, V. G.; Ortiz, J. V.; Foresman, J. B.; Cioslowski, J.; Stefanov, B. B.; Nanayakkara, A.; Challacombe, M.; Peng, C. Y.; Ayala, P. Y.; Chen, W.; Wong, M. W.; Andres, J. L.; Replogle, E. S.; Gomperts, R.; Martin, R. L.; Fox, D. J.; Binkley, J. S.; Defrees, D. J.; Baker, J.; Stewart, J. P.; Head-Gordon, M.; Gonzalez, C.; Pople, J. A. *Gaussian 94*, revision E.2; Gaussian, Inc.: Pittsburgh, PA, 1995.
- Zerner, M. C. "Semiempirical Molecular Orbital Methods" in *Reviews of Computational Chemistry*; Lipkowitz, K. B., Boyd, D. B., Eds.; VCH Publishers Inc., New York, 1991; pp 313-365 and references therein.
- Bartocci, G.; Spalletti, A.; Becker, R. S.; Elisei, F.; Floridi, S.; Mazzucato, U. *J. Am. Chem. Soc.* **1999**, *121*, 1065.
- Wold, S. *Technometrics* **1978**, *20*, 397.
- Bartocci, G.; Masetti, F.; Mazzucato, U.; Marconi, G. *J. Chem. Soc., Faraday Trans. 2* **1984**, *80*, 1093.
- Hug, G.; Becker, R. S. *J. Chem. Phys.* **1976**, *65*, 55.
- Hudson, B. S.; Kohler, B. E. *J. Chem. Phys.* **1973**, *59*, 4984.
- Andrews, J. R.; Hudson, B. E. *J. Chem. Phys.* **1978**, *68*, 4587.
- Baraldi, I.; Momicchioli, F.; Ponterini, G. *J. Mol. Struct. (THEOCHEM)* **1984**, *110*, 187.
- Wismontski-Knittel, T.; Das, P. K. *J. Phys. Chem.* **1984**, *88*, 2803.
- Saltiel, J.; et al. *Org. Photochem.* **1973**, *3*, 1. Saltiel, J.; Charlton, J. L. in *Rearrangements in Ground and Excited States*; de Mayo, P., Ed.; Academic: New York, 1980; Vol. 3, pp 25-89.